Catechol siderophores repress the pyochelin pathway and activate the enterobactin pathway in Pseudomonas aeruginosa : an opportunity for siderophore-antibiotic 2 conjugates development

Véronique Gasser, Etienne Baco, Olivier Cunrath, Pamela Saint August, Quentin Perraud, Nicolas Zill, Christian Schleberger, Alexander Schmidt, Aurélie Paulen, Dirk Bumann, et al.

Catechol siderophores repress the pyochelin pathway and activate the enterobactin pathway in *Pseudomonas aeruginosa*: an opportunity for siderophore-antibiotic conjugates development

Running title: Ability of *P. aeruginosa* to acquire iron via catechols

Véronique Gasser[1,2#], Etienne Baco[1,2], Olivier Cunrath[1,2,¶], Pamela Saint August[3], Quentin Perraud[1,2], Nicolas Zill[1,2], Christian Schleberger[3], Alexander Schmidt[3], Aurélie Paulen[1,2], Dirk Bumann[3], Gaëtan L. A. Mislin[1,2], Isabelle J. Schalk[1,2#]

1. Université de Strasbourg, ESBS, F-67413 Illkirch, France
2. CNRS, UMR 7242, F-67413 Illkirch, France
3. Focal Area Infection Biology, Biozentrum, University of Basel, Basel, Switzerland

To whom correspondence should be addressed: Isabelle J. Schalk, UMR 7242, ESBS, 300 Blvd Sébastien Brant, CS 10413, F-67412 Illkirch, Strasbourg, France. Tel: 33 3 68 85 47 19; Fax: 33 3 68 85 48 29; E-mail: isabelle.schalk@unistra.fr

Véronique Gasser, UMR 7242, ESBS, Blvd Sébastien Brant, CS 10413, F-67412 Illkirch, Strasbourg, France. Tel: 33 3 68 85 44 46; Fax: 33 3 68 85 48 29; E-mail: veronique.gasser@unistra.fr

¶ Currently at the Biozentrum, University of Basel, Basel, Switzerland

This article has been accepted for publication and undergone full peer review but has not been through the copyediting, typesetting, pagination and proofreading process, which may lead to differences between this version and the Version of Record. Please cite this article as doi: 10.1111/1462-2920.13199

ABSTRACT

Previous studies have suggested that antibiotic vectorization by siderophores (iron chelators produced by bacteria) considerably increases the efficacy of such drugs. The siderophore serves as a vector: when the pathogen tries to take up iron via the siderophore, it also takes up the antibiotic. Catecholates are among the most common iron-chelating compounds used in synthetic siderophore-antibiotic conjugates. Using RT-qPCR and proteomic approaches, we showed that the presence of catecholate compounds in the medium of *Pseudomonas aeruginosa* led to strong activation of the transcription and expression of the outer membrane transporter PfeA, the ferri-enterobactin importer. ^{55}Fe uptake assays on bacteria with and without PfeA expression confirmed that catechol compounds imported iron into *P. aeruginosa* cells via PfeA. Uptake rates were between 0.3 x 10^3 and 2 x 10^3 Fe atoms/bacterium/min according to the used catechol siderophore in iron-restricted medium, and remained as high as 0.8 x 10^3 Fe atoms/bacterium/min for enterobactin, even in iron-rich medium. RT-qPCR and proteomic approaches showed that in parallel to this switching on of PfeA expression, a repression of the expression of pyochelin (PCH) pathway genes (PCH being one of the two siderophores produced by *P. aeruginosa* for iron acquisition) was observed.

INTRODUCTION

The emergence of resistant and, in some cases pan-resistant (resistant to all the antibiotics currently available) bacteria has led to an urgent need to discover new bactericidal molecules with different targets and innovative strategies for preserving or increasing the efficacy of known antibiotics. In recent years, a number of reviews have highlighted the possible use of bacterial iron uptake pathways as a Trojan horse strategy for promoting the transport of drugs into bacteria, thereby increasing their efficacy (Ji et al., 2012b; Rebuffat, 2012; Page, 2013; Mislin and Schalk, 2014). Iron is a cofactor in many important biological processes, and it is therefore an essential nutrient for bacterial growth and infectious processes (Ratledge and Dover, 2000). One of the most common strategies for obtaining iron used by bacteria involves siderophores, small organic iron chelators (MW between 200 and 2000 Da; (Hider and Kong, 2011)). These molecules are synthesized by bacteria and have a high affinity for iron. They are released into the environment, where they scavenge iron highly efficiently before being taken up again by the bacteria, resulting in the transport of the iron they carry to the bacterial cytoplasm (Schalk et al., 2012; Schalk and Guillon, 2013). Antibiotics can be attached to siderophores in a Trojan horse strategy resulting in the delivery of the conjugates to the bacterial cytoplasm via siderophore-mediated iron uptake pathways.

In Gram-negative bacteria, the ferri-siderophore complexes formed in the environment surrounding the bacterium are transported back across the bacterial outer membrane by specific TonB-dependent transporters (TBDTs), the uptake activity of which is regulated by the inner membrane protein TonB (Schalk et al., 2012). They are further transported across the inner membrane by specific ABC transporters or protonmotive force-dependent permeases (Schalk and Guillon, 2013). The iron is generally then released from the siderophores in the bacterial cytoplasm, through a process involving both iron reduction and an enzymatic degradation or modification of the siderophores (for a review see (Schalk and Guillon, 2013)).

In some siderophore pathways, a different sequence of events occurs: for example, during iron uptake via pyoverdine (PVD) or citrate in *P. aeruginosa*, the iron is released from the siderophore in the periplasm, and only the iron is transported further into the cytoplasm, by an ABC transporter (Greenwald et al., 2007; Marshall et al., 2009; Brillet et al., 2012; Schalk and Guillon, 2013).

Most bacteria acquire iron by producing their own siderophores, but they can also use siderophores from other microorganisms (siderophore piracy). *P. aeruginosa*, an opportunist pathogen, used as a model organism in this study, produces two major siderophores, pyoverdine (PVD) and pyochelin (PCH). However, it can also use many xenosiderophore (not produced by the bacterium itself) like pyoverdines from other pseudomonads, enterobactin (Poole et al., 1990), cepabactin (Mislin et al., 2006), mycobactin and carboxymycobactin (Llamas et al., 2008), desferrichrysin, desferricrocin, coprogen (Meyer, 1992)), vibriobactin, aerobactin, fungal siderophores (ferrichrome (Llamas et al., 2006), deferrioxamines (Vasil and Ochsner, 1999; Llamas et al., 2006), and natural chelators, such as citrate (Cox, 1980; Harding and Royt, 1990), (for reviews see (Poole and McKay, 2003; Cornelis and Dingemans, 2013)).

Many studies have shown that siderophore iron uptake pathways can be used to transport antibiotics into bacteria (Mollmann et al., 2009; Ji et al., 2012b; Page, 2013; Mislin and Schalk, 2014). Microorganisms have themselves developed siderophore-antibiotic conjugates known as sideromycins (Braun and Braun, 2002; Braun et al., 2009; Mislin and Schalk, 2014), in which the antibiotic moiety is connected to the siderophore via a spacer arm. The archetypal conjugates of this type are albomycins (Benz et al., 1982; Braun and Braun, 2002; Mislin and Schalk, 2014), ferrimycins (Bickel et al., 1965), danomycins (Tsukiura et al., 1964), salmycins (Tsukiura et al., 1964) and certain microcins (de Lorenzo, 1984; de Lorenzo et al., 1984; Thomas et al., 2004; Destoumieux-Garzon et al., 2006; Nolan and

Walsh, 2008). These natural siderophore-antibiotic conjugates can chelate iron(III) and are then transported into the target bacterium via the siderophore-dependent iron uptake pathways. This energy-coupled transport across the bacterial membranes greatly increases the antibiotic efficacy of sideromycins: their minimal inhibitory concentration is often at least two orders of magnitude lower than that of the antibiotic without the siderophore, which enters the cell by diffusion (Braun et al., 2009). Trojan horse strategies based on the use of bacterial iron uptake pathways are, therefore, currently considered to be a promising approach for the treatment of infection. Several research teams have developed different synthetic siderophore-antibiotic conjugates (Rivault et al., 2007; Page et al., 2010; Noel et al., 2011; Ji et al., 2012b; Ji et al., 2012a; Milner et al., 2013; Page, 2013; Wencewicz et al., 2013; Wencewicz and Miller, 2013; Fardeau et al., 2014; Zheng and Nolan, 2014; Ji and Miller, 2015), some of which have potentially useful antibiotic activities.

However, for such Trojan horse strategies to be effective, the target bacteria must prefer to use xenosiderophores present in their environment rather than producing their own siderophores to obtain iron. In this context, it is vital to have a precise understanding of the ability of bacteria to sense the presence of xenosiderophores (or sideromycins in a Trojan horse strategy) in their environment and to switch from one siderophore pathway to another for iron acquisition. Catecholate siderophores are the iron-chelating compounds most frequently tethered to various antibiotics (Ji et al., 2012a; Wencewicz and Miller, 2013; Fardeau et al., 2014; Zheng and Nolan, 2014; Chairatana et al., 2015). In this study, we therefore evaluated the capacity of *P. aeruginosa* to use several catechol xenosiderophores in conditions of iron limitation: enterobactin (a well known siderophore produced by *Escherichia coli*, used here as a reference), protochelin and azotochelin (siderophores produced by *Azotobacter vinelandii* (Knosp et al., 1984; Cornish and Page, 2000)) and two synthetic chelators (the tris-catechol vector, TCV and the bis-catechol vector, BCV (Baco et

al., 2014)), which could potentially be used for the vectorization of antibiotics for transport into *P. aeruginosa* cells (Figure 1). We show here that when *P. aeruginosa* cells are grown in the presence of catechol compounds, the expression of the TBDT PfeA (the enterobactin outer membrane transporter) is highly activated and the expression of the genes encoding for proteins involved in the endogenous PCH iron uptake pathway is repressed. Using ^{55}Fe uptake assays, we show that iron is transported by these catechol compounds *via* PfeA, into *P. aeruginosa* cells.

RESULTS

Enterobactin, azotochelin, protochelin, BCV and TCV induce the expression of the outer membrane transporter PfeA. *P. aeruginosa* is known to be able to sense xenosiderophores in its extracellular environment, and the detection of these molecules leads to an upregulation of the genes encoding the corresponding ferrisiderophore uptake proteins (Dean and Poole, 1993; Llamas et al., 2008; Llamas et al., 2014). We used RT-qPCR and proteomic approaches to investigate whether the presence of catecholate chelators in the growth medium activated the transcription of one or more siderophore TBDTs in *P. aeruginosa*. For both approaches, experiments were carried out with PAO1 ATCC15692 and the corresponding PVD- and PCH-deficient Δ*pvdF*Δ*pchA* strain (Table S1 in the Supporting Information) grown in LB or iron-deficient CAA medium, with or without supplementation with 10 µM of enterobactin (the reference compound), azotochelin, protochelin, BCV or TCV.

We studied 10 genes in RT-qPCR experiments: 7 genes corresponding to TBDTs (*piuA, pirA, pfeA, cirA, fvbA, pfuA* and PA0434) potentially involved in iron acquisition via catechol chelators according to the annotation of the *P. aeruginosa* PAO1 genome (Winsor et al., 2011), the *fpvA* and *fptA* genes to assess changes in the transcription of the genes encoding the PVD and PCH TBDTs, and the housekeeping gene *uvrD,* which was used for normalization. RT-qPCR demonstrated a large increase in transcript levels for *pfeA* (Figure 2) but not for any of the other TBDT genes tested (fold-changes of less than 7 for these other genes; Figure S1 in the Supporting Information) in the presence of enterobactin and the other four catecholate chelators tested. In the iron-deficient CAA medium, all five molecules tested strongly activated the transcription of *pfeA,* even in the wild-type strain PAO1, which produced and secreted large amounts of the endogenous siderophores, PVD and PCH (Cunrath et al., 2015a). TCV and protochelin were the most effective activators of *pfeA* transcription (3,000- and 4,500-fold changes in PAO1 and Δ*pvdF*Δ*pchA,* respectively), followed by protochelin, enterobactin (1,400-fold change), and azotochelin, with BCV the

least effective molecule (520- and 810-fold changes in PAO1 and Δ*pvdF*Δ*pchA*, respectively). In LB medium (containing about 4 µM iron (Cunrath et al., 2015a)), TCV, protochelin and enterobactin were able to promote *pfeA* transcription in both strains tested, with fold-changes of between 100 and 700 for TCV (Figure 2F). In LB medium, TCV was again the most effective compound for the activation of *pfeA* transcription. This activation of *pfeA* transcription in LB medium strongly suggested that *P. aeruginosa* made use of the enterobactin pathway to acquire iron even in iron-rich media, such as LB, if tris-catechol siderophores were present. The proteomic investigation was carried out on the wild-type PAO1 strain grown in CAA medium in the presence of enterobactin, BVC or TCV (Figure 3). It clearly demonstrated an activation of expression for the PfeA gene but for no other TBDT gene (Figure 3A).

In conclusion, RT-qPCR and proteomic investigations showed strong induction of the transcription and expression of *pfeA* in the presence of catechol chelators in iron-deficient and iron-rich media.

Enterobactin, azotochelin, protochelin, BCV and TCV can transport iron into P. aeruginosa cells via the TBDT PfeA. The activation of *pfeA* transcription and expression in the presence of the various catechol siderophores strongly suggests that these chelators transport iron into *P. aeruginosa* cells via this TBDT. We therefore assessed the ability of a mutant with a *pfeA* deletion to transport and accumulate ^{55}Fe in the presence of the various catechol siderophores.

In the first experiment (Figure 4A-4E), we prevented iron uptake by the endogenous siderophores by using the PCH- and PVD-negative *P. aeruginosa* mutant Δ*pvdF*Δ*pchA* and its *pfeA* deletion mutant derivative Δ*pvdF*Δ*pchA*Δ*pfeA,* grown in the presence of 10 µM enterobactin to induce PfeA expression. We also repeated all the ^{55}Fe uptake experiments

with cells subjected to pretreatment with the protonophore CCCP (Figure 4A-4E), which inhibits the protonmotive force of the bacteria, thereby preventing any TonB-dependent uptake (Clément et al., 2004). ^{55}Fe uptake was observed in Δ*pvdF*Δ*pchA* cells (shown in black in Figure 4A-4E) in the presence of the five molecules tested, but not in cells that had been treated with CCCP (shown in green in Figure 4A-4E). Thus, none of the five catechol-^{55}Fe complexes tested were able to diffuse across the outer membrane: the iron uptake observed was mediated exclusively by TBDTs. A complete inhibition of iron uptake was also observed for the *pfeA* mutant in the presence of enterobactin-^{55}Fe, protochelin-^{55}Fe and TCV-^{55}Fe (shown in red in Figure 4A, 4C and 4E), as shown by comparison with the Δ*pvdF*Δ*pchA* strain expressing PfeA, indicating that these three compounds transport iron into *P. aeruginosa* cells *via* PfeA only, with no other TBDT able to perform this function. In the presence of BCV and, to a lesser extent, azotochelin (Figure 4D and 4B), the inhibition of ^{55}Fe uptake in Δ*pvdF*Δ*pchA*Δ*pfeA* cells was incomplete, suggesting the involvement of another TBDT, in addition to PfeA, in iron acquisition by these two bis-catechol compounds. Iron uptake was restored by the complementation of Δ*pvdF*Δ*pchA*Δ*pfeA* with pMMB190*pfeA,* a pMMB derivative carrying the *pfeA* gene for all five catecholate compounds tested (shown in blue in Figure 4A-4E).

As all the ^{55}Fe uptake assays with the different catechol siderophores were carried out with enterobactin as the inducer of *pfeA* expression, the expression levels of this protein are equivalent in all the uptake assays using PAO1 in Figures 4A-4E. Therefore, the ^{55}Fe transport efficiency of the different catecholate compounds can be compared: uptake rates of 2 x 10^3 Fe atoms/bacterium/min were recorded in the presence of enterobactin as siderophore, 1.3 x 10^3 Fe atoms/bacterium/min in the presence of azotochelin, 0.6 x 10^3 in the presence of protochelin or BCV and 0.3 10^3 Fe atoms/bacterium/min for TCV. In these experimental

conditions, TCV appears about 7 times less efficient than enterobactin for ^{55}Fe uptake in *P. aeruginosa.*

We then compared these uptake rates obtained with PVD- and PCH-deficient Δ*pvdF*Δ*pchA* cells grown in conditions of iron limitation with those obtained when siderophore-producing PAO1 cells were grown in iron-rich media (Figure 5 and Table 1). The idea here was to compare ^{55}Fe uptake by catecholate compounds in more favorable (iron-restricted growth conditions with a strain unable to produce any endogenous siderophore) and less favorable conditions (iron-rich growth conditions with a strain able to produce two endogenous siderophores). In addition, we also investigated the effect of (i) a lack of induction of PfeA expression (black bares in Figure 5), (ii) induction with the siderophore enterobactin (gray bares in Figure 5) and (iii) induction with the catechol chelator used in the ^{55}Fe uptake assays (white bares in Figure 5), which lead to the induction of the transporter with different efficiencies according to Figure 2.

A significant ^{55}Fe uptake *via* PfeA was observed only when the bacteria were grown in the presence of a catechol chelator inducing PfeA expression (Figure 5), confirming again that this TBDT must be expressed to observe any ^{55}Fe uptake in the presence of such compounds. However, this rule was not respected in the case PAO1 cells grown in LB with protochelin and TCV used as siderophores. The second interesting point is an efficient iron transport via enterobactin, azotochelin and BCV even in PVD- and PCH-producing *P. aeruginosa* cells grown in iron-rich medium. At last, iron uptake rates did not differ significantly between cells in which PfeA expression was induced with enterobactin and cells in which PfeA expression was induced with the siderophores used for ^{55}Fe uptake assays, despite the high capacity of compounds such as TCV to induce PfeA expression (Figure 2F). This apparent absence of connection between the level of PfeA expression and iron uptake

rates may be due to differences in siderophores recognition efficiencies with the different proteins of the enterobactin iron uptake pathway in *P. aeruginosa*.

Thus, all the five catechol compounds transported iron into *P. aeruginosa* cells via PfeA, with enterobactin being the more efficient. The uptake rates could reach with enterobactin 1306 ± 220 Fe atoms/bacterium/min in *P. aeruginosa* cells unable to produce siderophores grown in iron-deficient medium, and it remained as high as 827 ± 64 Fe atoms/bacterium/min, even in a PVD- and PCH-producing strain grown in iron-rich medium (Figure 5 and Table 1).

Enterobactin, azotochelin, protochelin, BCV and TCV repress the expression of the PCH pathway, but not that of the PVD pathway. In parallel with the induction of PfeA expression, proteomic analyses on *P. aeruginosa* cells grown in iron-deficient medium in the presence of 10 µM enterobactin, BCV or TCV showed a repression of the expression of the genes involved in PCH biosynthesis (*pchA*, *pchB*, *pchC*, *pchD*, *pchE*, *pchF* and *pchG*), the genes encoding the outer and inner membrane importers of PCH-Fe (*fptA* and *fptX*, respectively) and the *pchH* and *pchI* genes of the PCH locus, the functions of which are unknown (Figure 3B). No effect on the expression of the genes of the PVD locus was observed. Since *P. aeruginosa* cells produce no PVD and PCH in LB (an iron-rich medium; (Cunrath et al., 2015a)), the repression of PCH pathway genes in the presence of catecholate compounds was observed only in conditions of iron limitation (CAA medium). RT-qPCR experiments confirmed that, in conditions of iron limitation, the presence of catechol compounds in the growth medium of *P. aeruginosa* clearly repressed the transcription of *pchE* (a non-ribosomal peptide synthetase involved in PCH biosynthesis), *fptA* and *fptX* (Figure 6A), with an 80 % decrease in the fold–changes recorded. Again, no repression of transcription was observed for the genes of the PVD pathway (*fpvA*, encoding the TBDT; *fpvF*, encoding a periplasmic

binding protein involved in ferri-PVD import and *pvdJ*, encoding an enzyme involved in PVD biosynthesis; Figure 6B).

We investigated the timing of this repression using *P. aeruginosa* cells expressing mCherry-tagged PchE or FptX (*pchEmcherry* and *fptXmcherry*, Table S1 in Supplemental Information). The constructions of these strains have been described previously (Cunrath et al., 2015b; Gasser et al., 2015). Chromosomal insertion of *mcherry* was chosen to obtain physiological protein expression levels. The insertion of *mcherry*, by allelic exchange, into wild-type PAO1 produced strains expressing mCherry fused to the C-terminus of either FptX (*fptXmcherry* strain) or PchE (*pchEmcherry* strain). We monitored the growth of these two strains in iron-depleted CAA medium after addition of 200 µM enterobactin, BCV or TCV, by measuring optical density at 600 nm upon time (Figure 7). These two strains carrying the fusion proteins grew as well as the parental strains PAO1 and the addition of the catechol compounds stimulated bacterial growth, a feature commonly observed with siderophores (Youard et al., 2007). After 8 h culture, PchE-mCherry and FptX-mCherry were already expressed in *P. aeruginosa* cells, and a clear repression of PchE-mCherry and FptX-mCherry expression was observed, beginning about one hour after the addition of catechol chelators to the growth medium. This repression was most effective with TCV and least effective with BCV, and persisted over about 20 h of culture.

This switching off of the PCH pathway was confirmed by carrying out PCH-^{55}Fe uptake assays (Figure 4F) on *P. aeruginosa* cells grown in the presence or absence of BCV or TCV. ^{55}Fe uptake via PCH was observed for bacteria grown in the presence of BCV or TCV, indicating that the repression of the PCH pathway documented by proteomic and RT-qPCR studies was not total, with the bacteria still able to acquire iron via PCH. However, ^{55}Fe uptake was clearly slower in cells grown in the presence of BCV or TCV (no plateau reached

after more than 15 min, Figure 4F curve in blue and red) than in cells grown in the absence of these compounds (plateau reached in about 3 min, Figure 4F curve in black).

These data show that the presence of catechol chelators in the growth medium of *P. aeruginosa* cells strongly represses the proteins of the PCH pathway. This repression occurred after about one hour of growth in planktonic conditions in CAA medium and was maintained throughout the rest of the culture period (20 h). This repression was not total, with the bacterium still able to acquire iron *via* the PCH siderophore.

DISCUSSION

In addition to its own siderophores, PVD and PCH, *P. aeruginosa* can use many siderophores produced by other microorganisms (Poole and McKay, 2003; Cornelis and Dingemans, 2013), consistent with the presence in the genome of this pathogen of more than 30 genes encoding TBDTs (Cornelis and Bodilis, 2009), which act as gates allowing the various ferrisiderophore complexes to enter bacteria. All these siderophore-dependent iron uptake pathways, indicating a high potential of this bacterium to adapt to different conditions of iron limitation, may be also considered as possible gates for the entry of siderophore-antibiotic conjugates in Trojan horse strategies.

We show here that the presence in the growth medium of catechol xenosiderophores (azotochelin and protochelin) or two synthetic chelators (BCV and TCV) that can be linked to antibiotics by click chemistry induced the expression of PfeA in *P. aeruginosa,* as previously reported for enterobactin (Dean and Poole, 1993). By contrast, no other TBDT was induced (Figure 2 and 3A). The efficiency of PfeA induction was highest for TCV, followed by protochelin, enterobactin, azotochelin and, finally BCV. Dean and Poole have shown that two genes, *pfeS* and *pfeR* (located immediately upstream from *pfeA),* encode the sensor kinase and response regulator, respectively, of a two-component system involved in regulating *pfeA* expression in response to enterobactin (Dean and Poole, 1993; Rodrigue et al., 2000). It is tempting to hypothesize that this two-component system is also involved in the regulation of *pfeA* expression in response to other catechol compounds. The sequence of PfeS suggests that it is an inner membrane protein (Dean and Poole, 1993), and further studies are required to gain insight into the mechanism of stimulus perception by this

protein: do the catechol compounds interact with this protein only after their transport into the bacterial periplasm or is another mechanism involved?

Despite the current lack of information concerning the molecular mechanisms underlying this stimulation of PfeA expression, the findings presented here already have interesting implications for the development of siderophore conjugates for Trojan horse strategies. First, the induction of PfeA expression (or switching on of the enterobactin pathway) was even significant in a wild-type PAO1 strain, indicating that, in the presence of catechol compounds, *P. aeruginosa* makes use of these molecules to obtain iron, despite its ability to produce the highly efficient siderophores PVD and PCH. In addition, the enterobactin pathway was switched on even in iron-rich medium (LB), leading to efficient iron uptake via this siderophore: 827 ± 64 Fe atoms/bacterium/min (Figure 5 and Table 1). The total iron content of bacteria in this medium is in the range of 810,000 Fe atoms/bacterium (Cunrath et al., 2015a).

This switching on of the enterobactin pathway was accompanied by a clear repression of the expression of the PCH pathway. However, the PCH pathway was not totally switched off (Figure 3F), the bacteria were still able to gain access to iron via PCH at any moment. This repression occurred as long as the bacteria were in contact with catechol chelators (Figure 7). No repression of the PVD pathway was observed. Interestingly, this hierarchy of iron uptake pathway expression reflects the affinity of the siderophores for ferric iron (10^{52} M^{-1}, $10^{30.8}$ M^{-1} and $10^{28.8}$ M^{-2} for enterobactin, PVD and PCH, respectively (Carrano and Raymond, 1979; Albrecht-Gary et al., 1994; Brandel et al., 2012)). Moreover iron chelation needs only one molecule of enterobactin or PVD per iron ion, but two molecules of PCH (2:1 -PCH:Fe-stoichiometry) to get an octahedral coordination. This suggests that, when several siderophores are present in the bacterial environment, the siderophore most successful

at chelating the available iron will scavenge it and deliver it to the microorganism. Consequently, the bacterium will specifically up regulate the expression of all the proteins required to obtain iron via this specific siderophore. In the presence of tricatechol chelators, PCH, which has a lower affinity for iron and chelates this metal with a 2:1 (PCH:Fe) stoichiometry, is probably not competitive for the chelation of this metal. Consequently, fewer PCH-Fe complexes are formed and transported into *P. aeruginosa* cells for activation of the PCH pathway via the cytoplasmic regulator PchR. By contrast, the presence of catechol-Fe complexes in the bacterial environment leads to the enterobactin pathway being switched on. Accordingly, in the development of siderophore-antibiotic conjugates, it may be important to design a siderophore moiety with a high enough affinity for iron to compete with the natural siderophores produced by the pathogen. Consequently, it is not surprising that compounds like siderophore conjugate monocarbams are poorly efficient in a Trojan horse strategy in *P. aeruginosa* infections (Tomaras et al., 2013; Kim et al., 2015). Such compounds have certainly affinities for iron lower than that of PCH and will not be competitive with the endogenous siderophores to provide iron to *P. aeruginosa* cells. Moreover, the iron chelation stoichiometry of such compounds is not 1:1 (siderophore:Fe) as for many natural siderophores; therefore iron loaded monocarbam conjugates may have complex tridimensional structures, which may be poorly recognized by TBDT for uptake.

^{55}Fe uptake assays demonstrated that *P. aeruginosa* cells used the TBDT PfeA to assimilate iron complexed with catechol compounds (Figure 4). Deletion of the *PfeA* gene abolished completely iron uptake by these compounds, with the exception of BCV, for which another, as yet unidentified TBDT must be involved in BCV-Fe assimilation. Previous studies have suggested that TBDTs are highly specific for iron

transport *via* one specific siderophore or structurally related siderophores, but never siderophores with very different chemical structures (for a review see (Schalk et al., 2012)). In *P. aeruginosa*, PfeA recognizes the ferric forms of the tris-catechol compounds enterobactin, azotochelin and TCV, but also the bis-catechol compounds protochelin and BCV at the bacterial cell surface and transports them across the outer membrane. Consequently, PfeA should be able to take up BCV-antibiotic and TCV-antibiotic conjugates.

In all conditions tested, enterobactin was the most efficient siderophore for iron uptake into *P. aeruginosa*, whereas protochelin with TCV were the least efficient (figures 4 and 5 and Table S4): 1306 ± 220 Fe atoms/bacterium/min for enterobactin and 273 ± 62 Fe atoms/bacterium/min for protochelin, for cells grown in iron-deficient conditions. Surprisingly, the uptake rates of the different catechol chelators did not reflect the ability of these compounds to induce PfeA expression. This apparent absence of connection between the level of PfeA expression and the rates of iron uptake mediated by catechol siderophores may be due to differences in the recognition and interaction efficiencies between these catecholate compounds and the different protein partners involved in iron acquisition via enterobactin in *P. aeruginosa*.

The iron uptake rates of enterobactin (1306 ± 220 Fe atoms/bacterium/min in iron-deficient medium and 827 ± 64 Fe atoms/bacterium/min in LB –Figure 5 and Table 1-) indicate that this siderophore should be able to transport large amounts of antibiotics in a Trojan horse strategy. The lower uptake rate of protochelin and TCV probably reflects difficulties interacting with one of the proteins involved in enterobactin uptake pathway: PfeA or another, unidentified partner. Iron uptake via enterobactin has been studied in detail in *E. coli* and involves transport across the outer membrane by the TBDT FepA, across the inner membrane by the ABC transporter

FepBCD and the release of the metal from the siderophore in the cytoplasm, via a mechanism involving iron reduction and siderophore hydrolysis (Raymond et al., 2003; Schalk and Guillon, 2013). This scenario does not seem to apply to *P. aeruginosa*, particularly as the operon containing *pfeA* in this bacterium contains only the PA2689 gene (downstream from *pfeA*) encoding a putative esterase (Winsor et al., 2011) with a typical signaling sequence suggesting a periplasmic distribution. No gene coding for an inner membrane transporter is present on the genome in the vicinity of *pfeA*, strongly suggesting that, as for iron acquisition *via* PVD, iron may be released from enterobactin and other catechol chelators in the periplasm of *P. aeruginosa*, rather than in the cytoplasm as in *E. coli*. However, further studies are required to obtain insight into the enterobactin pathway in *P. aeruginosa*, to identify the various protein partners and molecular mechanisms involved and to improve our understanding to facilitate the design of optimal catechol-antibiotic conjugates transported into *P. aeruginosa* cells with the same efficiency as for the natural siderophore enterobactin.

In conclusion, the development of Trojan horse strategies involves considering different parameters to ensure the design of siderophore-antibiotic compounds with a high probability of ensuring effective drug delivery. It involves the synthesis of siderophore-antibiotic conjugates having a very high affinity for iron, able to compete for this nutrient with the endogenous siderophores produced by the target bacterium. Moreover, it is crucial that the siderophore-antibiotic conjugates once loaded with iron can still be recognized by TBDTs with good affinities. Consequently, vectors having structural homologies with natural siderophores will be vectors with the highest probability to transport efficiently antibiotics into bacteria. At last, the development of such Trojan horse strategies also requires an excellent knowledge of the molecular mechanisms involved in ferrisiderophore uptake.

405 The data presented here indicate that enterobactin-antibiotic conjugates should
406 have a high potential for activating PfeA transcription, facilitating the transport of
407 large amounts of antibiotic into the bacteria (the transport of 800 to 2000 molecules of
408 antibiotic might be predicted). The high potential of TCV to activate the transcription
409 of PfeA is also of potential interest in such a study, to ensure that the catechol-
410 antibiotic conjugates remain close to the bacterial cell surface, ready to be transported.
411 An ideal catechol vector for the transport of antibiotics into bacteria would be a
412 compound able to activate the transcription of PfeA, like TCV, but able to ensure
413 transport with the uptake rate of enterobactin.
414

MATERIALS AND METHODS

Chemicals. The pyochelin (PCH) used for ^{55}Fe uptake assays was synthesized and purified as previously described (Zamri and Abdallah, 2000; Youard et al., 2007). Enterobactin was purchased from Sigma-Aldrich. Azotochelin (BCS), BCV and TCV were synthesized as previously described (Baco et al., 2014). The syntheses of protochelin (TCS) is described in the Supplementary Material.

Bacterial strains, plasmids and growth conditions. The *P. aeruginosa* and *Escherichia coli* strains and plasmids used in this study are listed in Table S1 in Supporting Information. *E. coli* strains were routinely grown in Luria-Bertani broth [(LB); Difco] at 37°C. *P. aeruginosa* strains were first grown overnight at 30°C in LB broth and were then washed, resuspended and cultured overnight at 30°C in iron-deficient CAA medium (casamino acid medium, composition: 5 g l^{-1} low-iron CAA (Difco), 1.46 g l^{-1} K_2HPO_4 $3H_2O$, 0.25 g l^{-1} $MgSO_4$ $7H_2O$. Carbenicillin was added at a concentration of 150 µg ml-1 when required.

Mutant construction. All enzymes for DNA manipulation were purchased from Fermentas and were used in accordance with the manufacturer's instructions. *E. coli* strain TOP10 (Invitrogen) was used as the host strain for all plasmids. The DNA fragments from *P. aeruginosa* used for cloning were amplified from the genomic DNA of the PAO1 strain with Phusion High-Fidelity DNA polymerase (ThermoFisher Scientific). The primers used are listed in Table S2 of the Supporting Information. As previously described (Guillon et al., 2012), the general procedure involved the insertion of the 700 bp flanking sequences on either side of the gene to be deleted into the pME3088 suicide vector (Voisard et al., 1994). Mutations in the chromosomal genome of *P. aeruginosa* were generated by transferring the suicide vector from *E. coli* TOP10 strains into the PAO1 strain and allowing the plasmid to integrate into the chromosome, with selection for tetracycline resistance. A second crossing-over event excising the vector was achieved by enrichment for tetracycline-sensitive cells, to

generate the corresponding mutants (Ye et al., 1995). All gene-deletion mutants were verified by PCR and sequencing.

For construction of the complementation plasmid encoding *pfeA* under the control of its own promoter, the gene was amplified from the chromosomal DNA of *P. aeruginosa* PAO1 by PCR with the pfeAatg-104F and pfeAstop+31R primers (Table S2 in Supporting Information). The PCR fragment was trimmed by digestion with *Eco*RI and *Hin*dIII and inserted between the sites for these enzymes in pMMB190 (Morales et al., 1991) and bacteria transformed with this vector.

Growth and quantification of fluorescence intensity. The cells were cultured overnight in CAA medium, pelleted by centrifugation and resuspended in fresh CAA medium and the resulting suspension was diluted so as to obtain an optical density at 600 nm of 0.01 units. We dispensed 200 µl of the suspension per well into a 96-well plate (Greiner, U-bottomed microplate). The plate was incubated at 30°C, with shaking, in a Tecan microplate reader (Infinite M200, Tecan) for measurements of OD_{600nm} and mCherry (excitation/emission wavelengths: 570 nm/610 nm) fluorescence at 30-minute intervals, for 40 h. After 8 h of culture, we added 200 µM enterobactin, BCV or TCV and continued measurements of OD_{600nm} and mCherry fluorescence. We calculated the mean of three replicates for each measurement.

Quantitative real-time PCR. Specific gene expression was measured by reverse transcription-quantitative PCR (RT-qPCR), as previously described (Gross and Loper, 2009). Briefly, overnight cultures of strains grown in LB or CAA medium were pelleted, resuspended and diluted in fresh medium to obtain an OD_{600nm} of 0.1 units. The cells were then incubated in the presence or absence of 10 µM enterobactin, azotochelin, protochelin, BCV and TCV, with vigorous shaking, at 30°C for 3 h (LB medium) or 8 h (CAA medium). An aliquot of 2.5 x 10^8 cells from this culture was added to two volumes of RNAprotect

Bacteria Reagent (Qiagen). Total RNA was extracted with an RNeasy Mini kit (Qiagen), treated with DNase (RNase-Free DNase Set, Qiagen) and purified with an RNeasy Mini Elute cleanup kit (Qiagen). We then reverse-transcribed 1 µg of total RNA with a High-Capacity RNA-to-cDNA Kit, in accordance with the manufacturer's instructions (Applied Biosystems). The amounts of specific cDNAs were assessed in a StepOne Plus instrument (Applied Biosystems) with Power Sybr Green PCR Master Mix (Applied Biosystems) and the appropriate primers (Table S1), with the *uvrD* mRNA used as an internal control. The transcript levels for a given gene in a given strain were normalized with respect to those for *uvrD* and are expressed as a ratio (fold-change) relative to the reference conditions.

***Proteomics analysis*.** For the digestion and cleanup steps, 10^9 *P. aeroginosa* cells were lysed in 50 µl lysis buffer (2% sodium deoxycholate, 0.1M ammoniumbicarbonate) and disrupted by two cycles of sonication for 20 seconds (Hielscher Ultrasonicator). Protein concentration was determined by BCA assay (Thermo Fisher Scientific) using a small sample aliquot.

Proteins were reduced with 5 mM TCEP (Tris (2-Carboxyethyl) phosphine Hydrochloride) for 10 min at 95°C, alkylated with 10 mM iodoacetamide for 30 min in the dark at room temperature. Sample were diluted with 0.1M ammoniumbicarbonate solution to a final concentration of 1% sodium deoxycholate before digestion with trypsin (Promega) at 37°C over night (protein to trypsin ratio: 50:1). After digestion, the samples were supplemented with TFA to a final concentration of 0.5% and HCl to a final concentration of 50 mM. Precipitated sodium deoxycholate was removed by centrifugation (15 minutes at 4°C at 14,000 rpm). Then, peptides were desalted on C18 reversed phase spin columns according to the manufacturer's instructions (Macrospin, Harvard Apparatus), dried under vacuum and stored at -80°C until further processing.

For the shotgun proteomics assays, 1 ug of peptides of each sample were subjected to LC–MS (Liquid chromatography-mass spectrometry) analysis using a dual pressure LTQ-Orbitrap

Elite mass spectrometer connected to an electrospray ion source (both Thermo Fisher Scientific) as described recently (Glatter et al., 2012) with a few modifications. In brief, peptide separation was carried out using an EASY nLC-1000 system (Thermo Fisher Scientific) equipped with a RP-HPLC column (75 µm × 45 cm) packed in-house with C18 resin (ReproSil-Pur C18–AQ, 1.9 µm resin; Dr. Maisch GmbH, Ammerbuch-Entringen, Germany) using a linear gradient from 95% solvent A (0.15% formic acid, 2% acetonitrile) and 5% solvent B (98% acetonitrile, 0.15% formic acid) to 28% solvent B over 120 min at a flow rate of 0.2 µl/min. The data acquisition mode was set to obtain one high resolution MS scan in the FT part of the mass spectrometer at a resolution of 240,000 full width at half-maximum (at m/z 400) followed by MS/MS scans in the linear ion trap of the 20 most intense ions using rapid scan speed. The charged state screening modus was enabled to exclude unassigned and singly charged ions and the dynamic exclusion duration was set to 30s. The ion accumulation time was set to 300 ms (MS) and 25 ms (MS/MS).

For label-free quantification, the generated raw files were imported into the Progenesis LC-MS software (Nonlinear Dynamics, Version 4.0) and analyzed using the default parameter settings. MS/MS-data were exported directly from Progenesis LC-MS in mgf format and searched against a decoy database the forward and reverse sequences of the predicted proteome from *P. aeruginosa* (SGD, download date: 04/03/2014, total of 23,971 entries) using MASCOT (version 2.4.0). The search criteria were set as follows: full tryptic specificity was required (cleavage after lysine or arginine residues); 3 missed cleavages were allowed; carbamidomethylation (C) was set as fixed modification; oxidation (M) as variable modification. The mass tolerance was set to 10 ppm for precursor ions and 0.6 Da for fragment ions. Results from the database search were imported into Progenesis and the final peptide feature list and the protein list containing the summed peak areas of all identified peptides for each protein, respectively, were exported from Progenesis LC-MS. Both lists

were further statically analyzed using an in-house developed R script (SafeQuant) and the peptide and protein false discovery rate (FDR) was set to 1% using the number of reverse hits in the dataset (Glatter et al., 2012).

Iron uptake. The protonophore CCCP (carbonyl cyanide *m*-chlorophenylhydrazone) was purchased from Sigma. $^{55}FeCl_3$ was obtained from Perkin Elmer Life and Analytical Sciences (Billerica, MA, USA), in solution, at a concentration of 71.1 mM, with a specific activity of 10.18 Ci/g. Siderophore-^{55}Fe complexes were prepared at ^{55}Fe concentrations of 20 µM, with a siderophore:iron (mol:mol) ratio of 20:1. Iron uptake assays were carried out as previously described for PVD-Fe transport (Schalk et al., 2001; Hoegy and Schalk, 2014), except that bacteria were grown in CAA medium in the presence or absence of 10 µM enterobactin or catechol chelator, to induce PfeA expression. The bacteria were then washed with 50 mM Tris-HCl pH 8.0, to eliminate the siderophores used to induce PfeA expression, and diluted to an OD_{600nm} of 1. Bacteria were then incubated in the presence of 200 nM chelator-^{55}Fe and the incorporation of radioactivity into the bacteria over time was monitored by filtration (Schalk et al., 2001; Hoegy and Schalk, 2014). The experiments were repeated with cells pretreated with 200 µM CCCP. This compound inhibits the protonmotive force across the bacterial cell membrane, thereby inhibiting TonB-dependent iron uptake (Clément et al., 2004). For the data presented in Table S3, the radioactivity incorporated into the bacteria was monitored after 15 minutes of incubation with the chelator-^{55}Fe complexes. ^{55}Fe uptake assays in the presence of PCH-^{55}Fe (200 nM) were carried out as for enterobactin except that the bacteria were harvest by centrifugation, as previously described (Hoegy et al., 2009; Hoegy and Schalk, 2014), and not by filtration to avoid an adsorption of PCH-^{55}Fe on the GFB filters.

ACKNOWLEDGMENTS

This work was partly funded by the *Centre National de la Recherche Scientifique* and grants from the ANR (*Agence Nationale de Recherche, IronPath* ANR-12-BSV8-0007-01). In addition, these results were generated as part of the work of the Translocation Consortium (www.translocation.com) supported by the Innovative Medicines Joint Undertaking under Grant Agreement no. 115525, through financial contributions from the European Union's Seventh Framework Programme (FP7/2007-2013) and contributions in kind from EFPIA companies. O. Cunrath held fellowships, initially from the French *Ministère de la Recherche et de la Technologie,* and then from the *Fondation pour la Recherche Médicale*.

REFERENCES

Albrecht-Gary, A.M., Blanc, S., Rochel, N., Ocacktan, A.Z., and Abdallah, M.A. (1994) Bacterial iron transport: coordination properties of pyoverdin PaA, a peptidic siderophore of *Pseudomonas aeruginosa*. *Inorg Chem* **33**: 6391-6402.

Baco, E., Hoegy, F., Schalk, I.J., and Mislin, G.L. (2014) Diphenyl-benzo[1,3]dioxole-4-carboxylic acid pentafluorophenyl ester: a convenient catechol precursor in the synthesis of siderophore vectors suitable for antibiotic Trojan horse strategies. *Org Biomol Chem* **12**: 749-757.

Benz, G., Schroeder, T., Kurz, J., Wuensche, C., Karl, W., G., S. et al. (1982) Konstitution der Desferriform der Albomycine δ1, δ2, ε. *Angew Chem* **94**: 552.

Bickel, H., Mertens, P., Prelog, V., Seibl, J., and Walser, A. (1965) Constitution of ferrimycin A1. *Antimicrob Agents Chemother (Bethesda)* **5**: 951-957.

Brandel, J., Humbert, N., Elhabiri, M., Schalk, I.J., Mislin, G.L.A., and Albrecht-Garry, A.-M. (2012) Pyochelin, a siderophore of *Pseudomonas aeruginosa*: Physicochemical characterization of the iron(III), copper(II) and zinc(II) complexes. *Dalton Trans* **41**: 2820-2834.

Braun, V., and Braun, M. (2002) Active transport of iron and siderophore antibiotics. *Curr Opin Microbiol* **5**: 194-201.

Braun, V., Pramanik, A., Gwinner, T., Koberle, M., and Bohn, E. (2009) Sideromycins: tools and antibiotics. *Biometals* **22**: 3-13.

Brillet, K., Ruffenach, F., Adams, H., Journet, L., Gasser, V., Hoegy, F. et al. (2012) An ABC transporter with two periplasmic binding proteins involved in iron acquisition in *Pseudomonas aeruginosa*. *ACS Chem Biol* **7**: 2036-2045.

Carrano, C.J., and Raymond, K.N. (1979) "Ferric Ion Sequestering Agents. 2. Kinetics and mechanism of iron removal from transferrin by enterobactin and synthetic tricatechols". *J Am Chem Soc* **101**: 5401-5404.

576 Chairatana, P., Zheng, T., and Nolan, E.M. (2015) Trageting Virulence: Salmochelin
577 modification tunes the antibacterial activity spectrum of beta-lactams for pathogen-selective
578 killing of *Escherichia coli*. *Chem Sci* **6**: 4458-4471.
579 Clément, E., Mesini, P.J., Pattus, F., Abdallah, M.A., and Schalk, I.J. (2004) The binding
580 mechanism of pyoverdin with the outer membrane receptor FpvA in *Pseudomonas*
581 *aeruginosa* is dependent on its iron-loaded status. *Biochemistry* **43**: 7954-7965.
582 Cornelis, P., and Bodilis, J. (2009) A survey of TonB-dependent receptors in fluorescent
583 pseudomonads. *Environ Microbiol Rep* **1**: 256-262.
584 Cornelis, P., and Dingemans, J. (2013) Pseudomonas aeruginosa adapts its iron uptake
585 strategies in function of the type of infections. *Front Cell Infect Microbiol* **3**: 75.
586 Cornish, A.S., and Page, W.J. (2000) Role of molybdate and other transition metals in the
587 accumulation of protochelin by *Azotobacter vinelandii*. *Appl Environ Microbiol* **66**: 1580-
588 1586.
589 Cox, C.D. (1980) Iron uptake with ferripyochelin and ferriccitrate by *Pseudomonas*
590 *aeruginosa*. *J bacteriol* **142**: 581-587.
591 Cunrath, O., Geoffroy, V.A., and Schalk, I.J. (2015a) Metallome of *Pseudomonas*
592 *aeruginosa*: a role for siderophores. *Environ Microbiol*.
593 Cunrath, O., Gasser, V., Hoegy, F., Reimmann, C., Guillon, L., and Schalk, I.J. (2015b) A
594 cell biological view of the siderophore pyochelin iron uptake pathway in *Pseudomonas*
595 *aeruginosa*. *Environ Microbiol* **17**: 171-185.
596 de Lorenzo, V. (1984) Isolation and characterization of microcin E492 from *Klebsiella*
597 *pneumoniae*. *Arch Microbiol* **139**: 72-75.
598 de Lorenzo, V., Martinez, J.L., and Asensio, C. (1984) Microcin-mediated interactions
599 between *Klebsiella pneumoniae* and *Escherichia coli* strains. *J Gen Microbiol* **130**: 391-400.

600 Dean, C.R., and Poole, K. (1993) Expression of the ferric enterobactin receptor (PfeA) of
601 *Pseudomonas aeruginosa*: involvement of a two-component regulatory system. *Mol*
602 *Microbiol* **8**: 1095-1103.
603 Destoumieux-Garzon, D., Peduzzi, J., Thomas, X., Djediat, C., and Rebuffat, S. (2006)
604 Parasitism of iron-siderophore receptors of *Escherichia coli* by the siderophore-peptide
605 microcin E492m and its unmodified counterpart. *Biometals* **19**: 181-191.
606 Fardeau, S., Dassonville-Klimpt, A., Audic, N., Sasaki, A., Pillon, M., Baudrin, E. et al.
607 (2014) Synthesis and antibacterial activity of catecholate-ciprofloxacin conjugates. *Bioorg*
608 *Med Chem* **22**: 4049-4060.
609 Gasser, V., Guillon, L., Cunrath, O., and Schalk, I.J. (2015) Cellular organization of
610 siderophore biosynthesis in *Pseudomonas aeruginosa*: Evidence for siderosomes. *J Inorg*
611 *Biochem* **148**: 27-34.
612 Glatter, T., Ludwig, C., Ahrne, E., Aebersold, R., Heck, A.J., and Schmidt, A. (2012) Large-
613 scale quantitative assessment of different in-solution protein digestion protocols reveals
614 superior cleavage efficiency of tandem Lys-C/trypsin proteolysis over trypsin digestion. *J*
615 *Proteome Res* **11**: 5145-5156.
616 Greenwald, J., Hoegy, F., Nader, M., Journet, L., Mislin, G.L.A., Graumann, P.L., and Schalk,
617 I.J. (2007) Real-time FRET visualization of ferric-pyoverdine uptake in *Pseudomonas*
618 *aeruginosa*: a role for ferrous iron. *J Biol Chem* **282**: 2987-2995.
619 Gross, H., and Loper, J.E. (2009) Genomics of secondary metabolite production by
620 *Pseudomonas* spp. *Nat Prod Rep* **26**: 1408-1446.
621 Guillon, L., El Mecherki , M., Altenburger, S., Graumann, P.L., and Schalk, I.J. (2012) High
622 cellular organisation of pyoverdine biosynthesis in *Pseudomonas aeruginosa:* localization of
623 PvdA at the old cell pole. *Environ Microbiol* **14**: 1982-1994.

624 Harding, R.A., and Royt, P.W. (1990) Acquisition of iron from citrate by *Pseudomonas*
625 *aeruginosa*. *J Gen Microbiol* **136**: 1859-1867.
626 Hider, R.C., and Kong, X. (2011) Chemistry and biology of siderophores. *Nat Prod Rep* **27**:
627 637-657.
628 Hoegy, F., and Schalk, I.J. (2014) Monitoring iron uptake by siderophores. *Methods Mol Biol*
629 **1149**: 337-346.
630 Hoegy, F., Lee, X., Noël, S., Mislin, G.L., Rognan, D., Reimmann, C., and Schalk, I.J. (2009)
631 Stereospecificity of the siderophore pyochelin outer membrane transporters in fluorescent
632 Pseudomonads. *J Biol Chem* **284**: 14949-14957.
633 Ji, C., and Miller, M.J. (2015) Siderophore-fluoroquinolone conjugates containing potential
634 reduction-triggered linkers for drug release: synthesis and antibacterial activity. *Biometals* **28**:
635 541-551.
636 Ji, C., Miller, P.A., and Miller, M.J. (2012a) Iron transport-mediated drug delivery: practical
637 syntheses and in vitro antibacterial studies of tris-catecholate siderophore-aminopenicillin
638 conjugates reveals selectively potent antipseudomonal activity. *J Am Chem Soc* **134**: 9898-
639 9901.
640 Ji, C., Juarez-Hernandez, R.E., and Miller, M.J. (2012b) Exploiting bacterial iron acquisition:
641 siderophore conjugates. *Future Med Chem* **4**: 297-313.
642 Kim, A., Kutschke, A., Ehmann, D.E., Patey, S.A., Crandon, J.L., Gorseth, E. et al. (2015)
643 Pharmacodynamic profiling of a siderophore-conjugated monocarbam in *Pseudomonas*
644 *aeruginosa*: assessing the risk for resistance and attenuated efficacy. *Antimicrob Agents*
645 *Chemother* **59**: 7743-7752.
646 Knosp, O., von Tigerstrom, M., and Page, W.J. (1984) Siderophore-mediated uptake of iron
647 in *Azotobacter vinelandii*. *J Bacteriol* **159**: 341-347.

Llamas, M.A., Imperi, F., Visca, P., and Lamont, I.L. (2014) Cell-surface signaling in *Pseudomonas*: stress responses, iron transport, and pathogenicity. *FEMS Microbiol Rev* **38**: 569-597.

Llamas, M.A., Sparrius, M., Kloet, R., Jimenez, C.R., Vandenbroucke-Grauls, C., and Bitter, W. (2006) The heterologous siderophores ferrioxamine B and ferrichrome activate signaling pathways in *Pseudomonas aeruginosa*. *J Bacteriol* **188**: 1882-1891.

Llamas, M.A., Mooij, M.J., Sparrius, M., Vandenbroucke-Grauls, C.M., Ratledge, C., and Bitter, W. (2008) Characterization of five novel *Pseudomonas aeruginosa* cell-surface signalling systems. *Mol Microbiol* **67**: 458-472.

Marshall, B., Stintzi, A., Gilmour, C., Meyer, J.M., and Poole, K. (2009) Citrate-mediated iron uptake in *Pseudomonas aeruginosa*: involvement of the citrate-inducible FecA receptor and the FeoB ferrous iron transporter. *Microbiology* **155**: 305-315.

Meyer, J.M. (1992) Exogenous siderophore-mediated iron uptake in *Pseudomonas aeruginosa*: possible involvement of porin OprF in iron translocation. *J Gen Microbiol* **138**: 951-958.

Milner, S.J., Seve, A., Snelling, A.M., Thomas, G.H., Kerr, K.G., Routledge, A., and Duhme-Klair, A.K. (2013) Staphyloferrin A as siderophore-component in fluoroquinolone-based Trojan horse antibiotics. *Org Biomol Chem* **11**: 3461-3468.

Mislin, G.L., and Schalk, I.J. (2014) Siderophore-dependent iron uptake systems as gates for antibiotic Trojan horse strategies against *Pseudomonas aeruginosa*. *Metallomics* **6**: 408-420.

Mislin, G.L.A., Hoegy, F., Cobessi, D., Poole, K., Rognan, D., and Schalk, I.J. (2006) Binding properties of pyochelin and structurally related molecules to FptA of *Pseudomonas aeruginosa*. *J Mol Biol* **357**: 1437-1448.

671 Mollmann, U., Heinisch, L., Bauernfeind, A., Kohler, T., and Ankel-Fuchs, D. (2009)
672 Siderophores as drug delivery agents: application of the "Trojan Horse" strategy. *Biometals*
673 **22**: 615-624.
674 Morales, V.M., Backman, A., and Bagdasarian, M. (1991) A series of wide-host-range low-
675 copy-number vectors that allow direct screening for recombinants. *Gene* **97**: 39-47.
676 Noel, S., Gasser, V., Pesset, B., Hoegy, F., Rognan, D., Schalk, I.J., and Mislin, G.L. (2011)
677 Synthesis and biological properties of conjugates between fluoroquinolones and a N3"-
678 functionalized pyochelin. *Org Biomol Chem* **9**: 8288-8300.
679 Nolan, E.M., and Walsh, C.T. (2008) Investigations of the MceIJ-catalyzed posttranslational
680 modification of the microcin E492 C-terminus: linkage of ribosomal and nonribosomal
681 peptides to form "trojan horse" antibiotics. *Biochemistry* **47**: 9289-9299.
682 Page, M.G. (2013) Siderophore conjugates. *Ann N Y Acad Sci* **1277**: 115-126.
683 Page, M.G., Dantier, C., and Desarbre, E. (2010) In vitro properties of BAL30072, a novel
684 siderophore sulfactam with activity against multiresistant gram-negative bacilli. *Antimicrob*
685 *Agents Chemother* **54**: 2291-2302.
686 Poole, K., and McKay, G.A. (2003) Iron acquisition and its control in *Pseudomonas*
687 *aeruginosa*: many roads lead to Rome. *Front Biosci* **8**: d661-686.
688 Poole, K., Young, L., and Neshat, S. (1990) Enterobactin-mediated iron transport in
689 *Pseudomonas aeruginosa. J Bacteriol* **172**: 6991-6996.
690 Ratledge, C., and Dover, L.G. (2000) Iron metabolism in pathogenic bacteria. *Annu Rev*
691 *Microbiol* **54**: 881-941.
692 Raymond, K.N., Dertz, E.A., and Kim, S.S. (2003) Enterobactin: an archetype for microbial
693 iron transport. *Proc Natl Acad Sci U S A* **100**: 3584-3588.
694 Rebuffat, S. (2012) Microcins in action: amazing defence strategies of *Enterobacteria*.
695 *Biochem Soc Trans* **40**: 1456-1462.

Rivault, F., Liébert, C., Burger, A., Abdallah, M.A., Schalk, I.J., and Mislin, G.L. (2007) Synthesis of pyochelin-norfloxacin conjuguates. *Bioorg Med Chem Lett* **17**: 640-644.

Rodrigue, A., Quentin, Y., Lazdunski, A., Mejean, V., and Foglino, M. (2000) Two-component systems in *Pseudomonas aeruginosa*: why so many? *Trends Microbiol* **8**: 498-504.

Schalk, I.J., and Guillon, L. (2013) Fate of ferrisiderophores after import across bacterial outer membranes: different iron release strategies are observed in the cytoplasm or periplasm depending on the siderophore pathways. *Amino Acids* **44**: 1267-1277.

Schalk, I.J., Mislin, G.L., and Brillet, K. (2012) Structure, function and binding selectivity and stereoselectivity of siderophore-iron outer membrane transporters. *Curr Top Membr* **69**: 37-66.

Schalk, I.J., Hennard, C., Dugave, C., Poole, K., Abdallah, M.A., and Pattus, F. (2001) Iron-free pyoverdin binds to its outer membrane receptor FpvA in *Pseudomonas aeruginosa*: a new mechanism for membrane iron transport. *Mol Microbiol* **39**: 351-360.

Thomas, X., Destoumieux-Garzon, D., Peduzzi, J., Afonso, C., Blond, A., Birlirakis, N. et al. (2004) Siderophore peptide, a new type of post-translationally modified antibacterial peptide with potent activity. *J Biol Chem* **279**: 28233-28242.

Tomaras, A.P., Crandon, J.L., McPherson, C.J., Banevicius, M.A., Finegan, S.M., Irvine, R.L. et al. (2013) Adaptation-based resistance to siderophore-conjugated antibacterial agents by *Pseudomonas aeruginosa*. *Antimicrob Agents Chemother* **57**: 4197-4207.

Tsukiura, H., Okanishi, M., Ohmori, T., Koshiyama, H., Miyaki, T., Kitazima, H., and Kawaguchi, H. (1964) Danomycin, a New Antibiotic. *J Antibiot (Tokyo)* **17**: 39-47.

Vasil, M.L., and Ochsner, U.A. (1999) The response of *Pseudomonas aeruginosa* to iron: genetics, biochemistry and virulence. *Mol Microbiol* **34**: 399-413.

Voisard, C., Bull, C., Keel, C., Laville, J., Maurhofer, M., Schnider, U. et al. (1994) Biocontrol of root diseases by Pseudomonas fluorescens CHAO: current concepts and

721 experimental approaches. In *Molecular Ecology of Rhizosphere Microorganisms*. O'Gara, F.,
722 Dowling, D.N., and Boesten (eds). Weinheim, Germany: VCH, pp. 67-89.
723 Wencewicz, T.A., and Miller, M.J. (2013) Biscatecholate-monohydroxamate mixed ligand
724 siderophore-carbacephalosporin conjugates are selective sideromycin antibiotics that target
725 *Acinetobacter baumannii*. *J Med Chem* **56**: 4044-4052.
726 Wencewicz, T.A., Long, T.E., Mollmann, U., and Miller, M.J. (2013) Trihydroxamate
727 siderophore-fluoroquinolone conjugates are selective sideromycin antibiotics that target
728 *Staphylococcus aureus*. *Bioconjug Chem* **24**: 473-486.
729 Winsor, G.L., Lam, D.K., Fleming, L., Lo, R., Whiteside, M.D., Yu, N.Y. et al. (2011)
730 *Pseudomonas* Genome Database: improved comparative analysis and population genomics
731 capability for *Pseudomonas* genomes. *Nucleic Acids Res* **39**: D596-600.
732 Ye, R.W., Haas, D., Ka, J.O., Krishnapillai, V., Zimmermann, A., Baird, C., and Tiedje, J.M.
733 (1995) Anaerobic activation of the entire denitrification pathway in *Pseudomonas aeruginosa*
734 requires Anr, an analog of Fnr. *J Bacteriol* **177**: 3606-3609.
735 Youard, Z.A., Mislin, G.L., Majcherczyk, P.A., Schalk, I.J., and Reimmann, C. (2007)
736 *Pseudomonas fluorescens* CHA0 produces enantio-pyochelin, the optical antipode of the
737 *Pseudomonas aeruginosa* siderophore pyochelin. *J Biol Chem* **282**: 35546-35553.
738 Zamri, A., and Abdallah, M.A. (2000) An improved stereocontrolled synthesis of pyochelin, a
739 siderophore of *Pseudomonas aeruginosa* and *Burkholderia cepacia*. *Tetrahedron* **56**: 249-256.
740 Zheng, T., and Nolan, E.M. (2014) Enterobactin-mediated delivery of beta-lactam antibiotics
741 enhances antibacterial activity against pathogenic *Escherichia coli*. *J Am Chem Soc* **136**:
742 9677-9691.
743

744 **TABLE**
745

	^{55}Fe atoms/bacterium/min				
	Enterobactin	Azotochelin	Protochelin	BCV	TCV
PAO1 in LB	827 ± 64	299 ± 33	98 ± 4	661 ± 32	145 ± 14
Δ*pvdF*Δ*pchA* in CAA	1306 ± 220	712 ± 126	273 ± 62	372 ± 68	363 ± 36

746

747 **Table 1: ^{55}Fe assimilation in *P. aeruginosa* PAO1 and Δ*pvdF*Δ*pchA* cells in the presence**
748 **of ^{55}Fe -loaded enterobactin, azotochelin, protochelin, BCV and TCV.** PAO1 was grown
749 in LB and the corresponding PVD- and PCH-deficient Δ*pvdF*Δ*pchA* strain in CAA medium.
750 Cells were grown with 10 µM of the catechol compound used for ^{55}Fe uptake to induce PfeA
751 expression. The bacteria were then washed with 50 mM Tris-HCl (pH 8.0) and transport
752 assays were initiated by adding the various catechol compounds loaded with ^{55}Fe to a
753 concentration of 200 nM. Samples (100 µl) were taken from the suspensions at various time
754 points and filtered; the radioactivity retained was measured. The results are expressed as
755 atoms of ^{55}Fe transported per bacterium per min (n = 3).

756

FIGURE LEGENDS

Figure 1: Structures of enterobactin (ENT), azotochelin (BCS), protochelin (TCS), bis-catechol vector (BCV) and tris-catechol vector (TCV).

Figure 2: Analysis of changes in the transcription of the *pfeA* gene. RT-qPCR was performed on RNA from *P. aeruginosa* PAO1 and the corresponding PVD- and PCH-deficient Δ*pvdF*Δ*pchA* cells grown in CAA or LB medium, with and without supplementation with 10 µM enterobactin, azotochelin, protochelin, BCV or TCV. The data are normalized relative to the reference gene *uvrD* and are representative of three independent experiments performed in triplicate (*n*=3).

Figure 3: Analysis of expression changes for TBDTs (panel A) and proteins of the PVD (panel B; green, blue and red crosses) and PCH (panel B; green, blue and red triangles) pathways. Proteomic analyses were performed on *P. aeruginosa* PAO1 cells grown in CAA supplemented or not with 10 µM enterobactin, BCV or TCV. Median values measured in CAA in the absence of any supplementation with catechol compounds were plotted against median values measured in CAA supplemented with either enterobactin (green symbols in panel A and B), BCV (blue symbols in panel A and B) and TCV (red symbols in panel A and B). Median values represent the median of the relative intensity of each protein, normalized against all detected proteins during shotgun analyses (n=3).

Figure 4: Panels A-E. Time-dependent ^{55}Fe assimilation in *P. aeruginosa* cells in the presence of ^{55}Fe-loaded enterobactin, azotochelin, protochelin, BCV and TCV. The PVD- and PCH-deficient Δ*pvdF*Δ*pchA* strain, its corresponding *pfeA* mutant (Δ*pvdF*Δ*pchA*Δ*pfeA*) and the complemented Δ*pvdF*Δ*pchA*(pME3088Δ*pvdF*) strain were

grown in CAA medium in the presence of 10 µM enterobactin, to induce PfeA expression. The bacteria were then washed with 50 mM Tris-HCl (pH 8.0) and transport assays were initiated by adding 200 nM enterobactin-^{55}Fe (**panel A**), azotochelin-^{55}Fe (**panel B**), protochelin-^{55}Fe (**panel C**), BCV-^{55}Fe (**panel D**) or TCV-^{55}Fe (**panel E**). Samples (100 µl) of the suspension were taken at various time points and filtered; the radioactivity retained was measured. The results are expressed as atoms of ^{55}Fe transported per bacterium. For **panels A-E**, the black and red lines correspond to ^{55}Fe uptake assays with Δ*pvdF*Δ*pchA* and Δ*pvdF*Δ*pchA*Δ*pfeA* cells respectively, both grown in the presence of enterobactin; in green: ^{55}Fe uptake assay with Δ*pvdF*Δ*pchA* cells grown in the presence of enterobactin and then treated with 200 µM CCCP (a protonophore), preventing TBDT-dependent transport; in blue: ^{55}Fe uptake assay with Δ*pvdF*Δ*pchA*(pME3088Δ*pvdF*) cells grown in the presence of enterobactin. **Panel F. Time-dependent ^{55}Fe assimilation in *P. aeruginosa* cells in the presence of PCH.** Δ*pvdF*Δ*pchA* cells were grown in CAA medium in the absence of chelator (gray) or in the presence of 10 µM BCV (dark blue) or TCV (purple), to induce PfeA expression. As above, the bacteria were then washed with 50 mM Tris-HCl (pH 8.0) and transport assays were initiated by adding 200 nM PCH-^{55}Fe. The experiments were repeated with the protonophore CCCP at a concentration of 200 µM (light blue and pink: Δ*pvdF*Δ*pchA* cells treated with CCCP after culture in the presence of 10 µM BCV and TCV, respectively). All the experiments in **panels A-F** were carried out three times, with similar results obtained in each case.

Figure 5: ^{55}Fe assimilation in *P. aeruginosa* PAO1 and Δ*pvdF*Δ*pchA* cells in the presence of ^{55}Fe -loaded enterobactin, azotochelin, protochelin, BCV and TCV. PAO1 was grown in LB and the corresponding PVD- and PCH-deficient Δ*pvdF*Δ*pchA* strain in CAA medium. Cells were grown without enterobactin supplementation to ensure an absence of PfeA

807 expression (black bars) or with 10 µM enterobactin (gray bars) or 10 µM of the catechol
808 compound used for ^{55}Fe uptake (white bars) to induce PfeA expression. The bacteria were
809 then washed with 50 mM Tris-HCl (pH 8.0) and transport assays were initiated by adding the
810 various catechol compounds loaded with ^{55}Fe to a concentration of 200 nM. Samples (100 µl)
811 were taken from the suspensions at various time points and filtered; the radioactivity retained
812 was measured. The results are expressed as atoms of ^{55}Fe transported per bacterium per min.
813 Data of Figure 5 are presented as well in Table S4 in Supplemental Information.
814
815 **Figure 6: A. Analysis of changes in transcription for the genes of the PCH pathway.** *fptA*
816 and *fptX* encode the outer and inner membrane transporters of PCH-Fe, respectively, and
817 *pchE* encodes an NRPS involved in PCH biosynthesis. RT-qPCR was performed on *P.*
818 *aeruginosa* PAO1 grown in CAA medium with or without 10 µM enterobactin, azotochelin,
819 protochelin, BCV or TCV (NI for not induced). **B. Analysis of changes in the transcription**
820 **of genes of the PVD pathway.** *fpvA* encodes the TBDT of PVD-Fe, *fpvF* encodes a
821 periplasmic binding protein involved in PVD-Fe uptake, *pvdI* encodes an non-ribosomal
822 peptide synthetases involved in PVD biosynthesis. As for panel B, RT-qPCR was performed
823 on *P. aeruginosa* PAO1 cells grown in CAA medium with or without 10 µM enterobactin,
824 azotochelin, protochelin, BCV or TCV (NI for not induced). For both panels, the data were
825 normalized relative to the reference gene *uvrD* and are representative of three independent
826 experiments performed in triplicate (n=3).
827
828 **Figure 7: Monitoring of PchE-mCherry (panel A) and FptX-mCherry (panel B)**
829 **fluorescence during bacterial growth in the presence and absence of enterobactin, BCV**
830 **or TCV.** Fresh CAA medium was inoculated with *pchEmcherry* and *fptXmcherry* cells grown
831 in the same medium, and the resulting suspension was dispensed into the wells of a 96-well

plate. For both panels, after 8 h of growth, 200 µM enterobactin (●), BCV (□) or TCV (▲) was added; the control experiment with no siderophore addition is shown in black (black line with no symbols). OD_{600nm} measurements were used to assess growth over time. The fluorescence of mCherry was measured by excitation at 570 nm, with monitoring of the emission of fluorescence at 610 nm. These measurements were performed at 30-minute intervals, in a Tecan microplate reader incubated at 30°C, with shaking. Each curve corresponds to the mean of three replicates

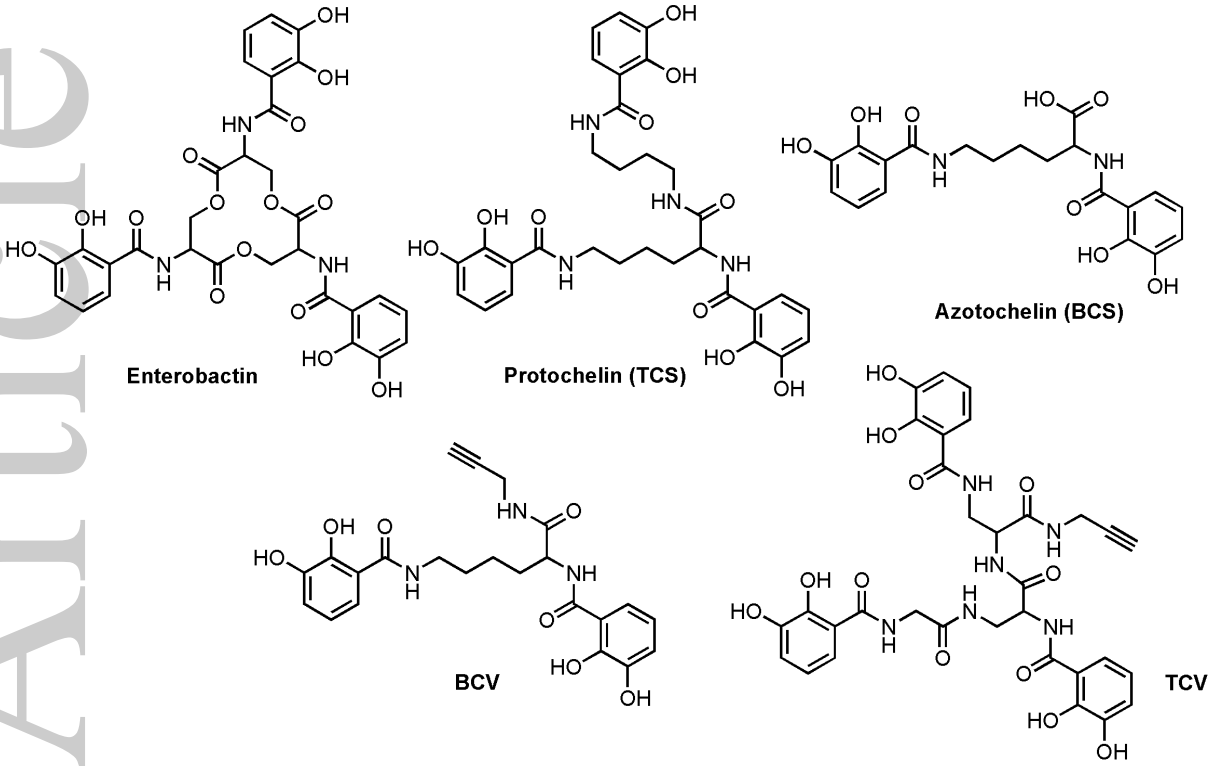

840

841 **EMI_13199_F1**

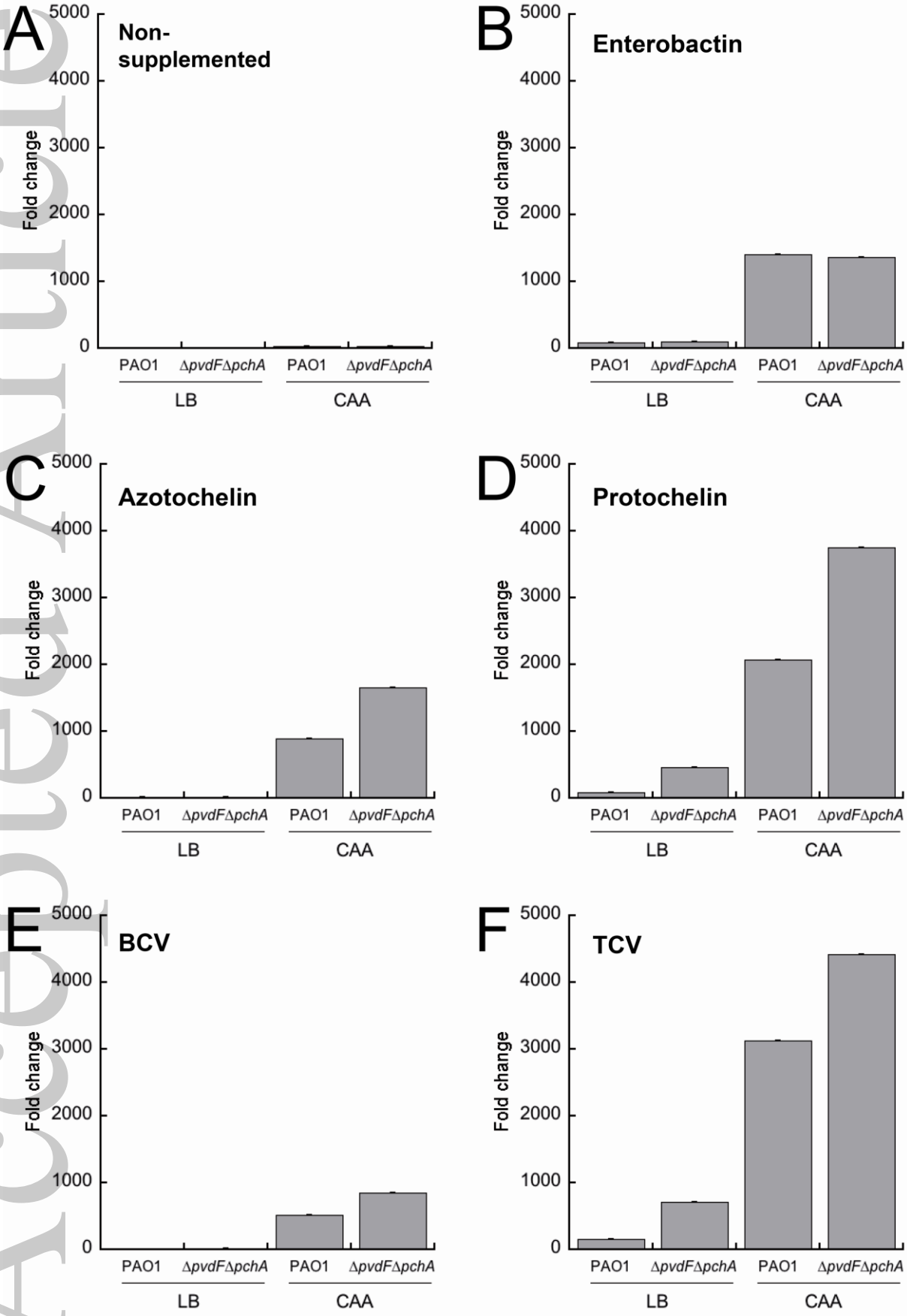

842

843 **EMI_13199_F2**

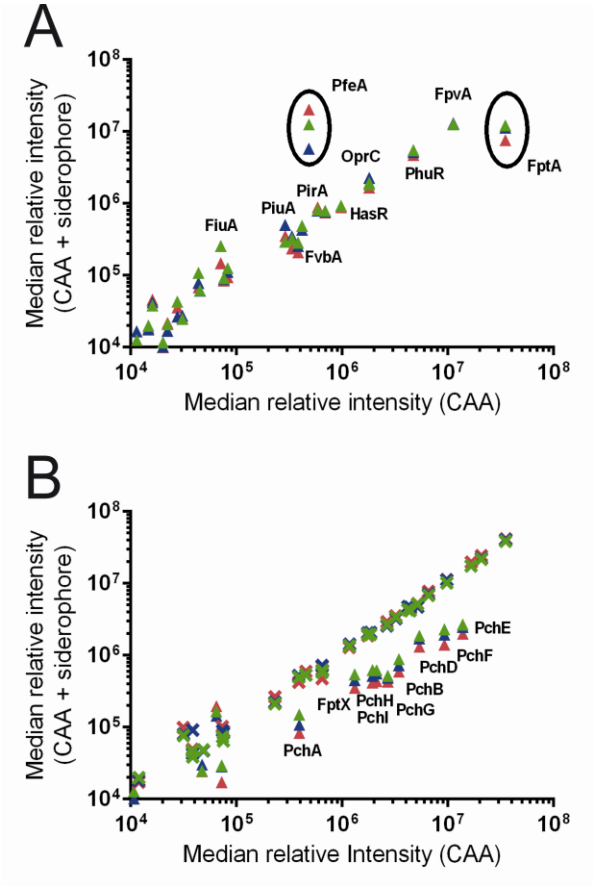

EMI_13199_F3

847

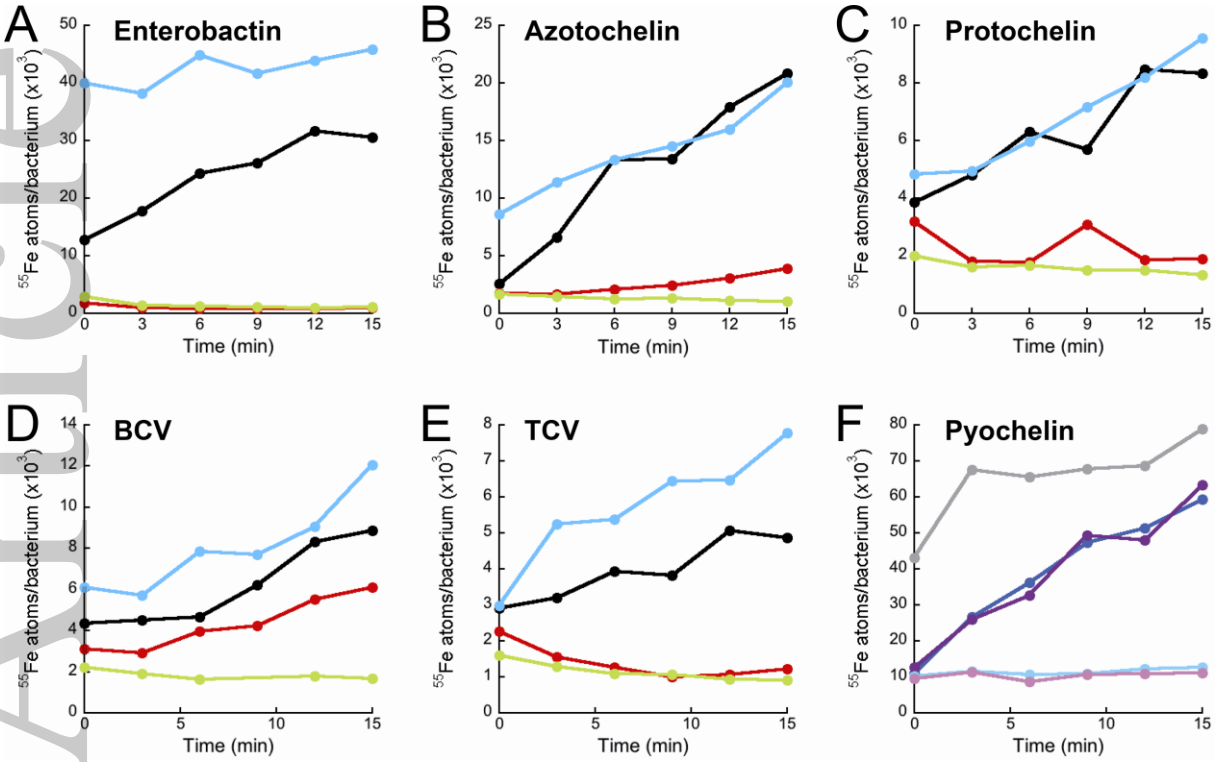

848 **EMI_13199_F4**

849

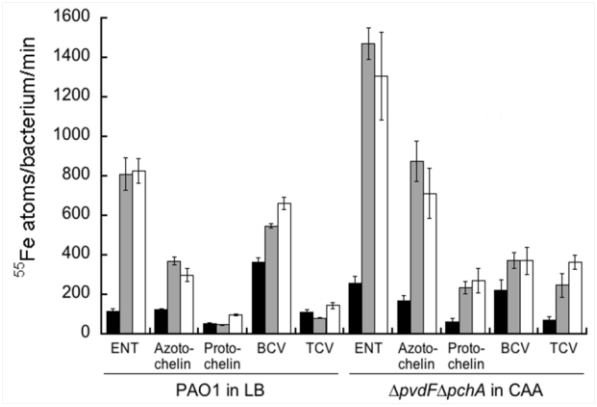

850

851 **EMI_13199_F5**

852

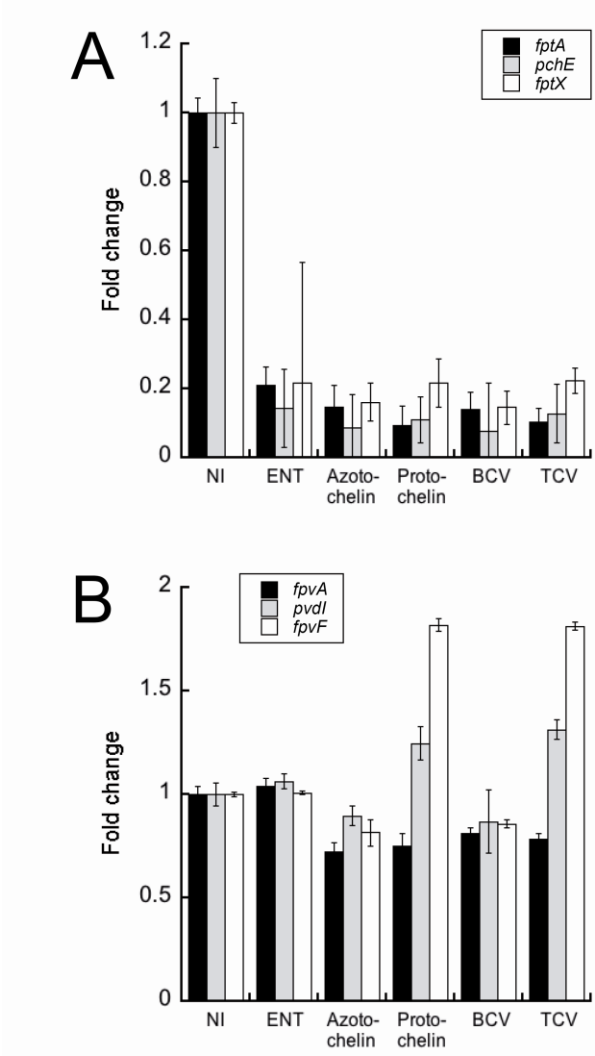

853 **EMI_13199_F6**

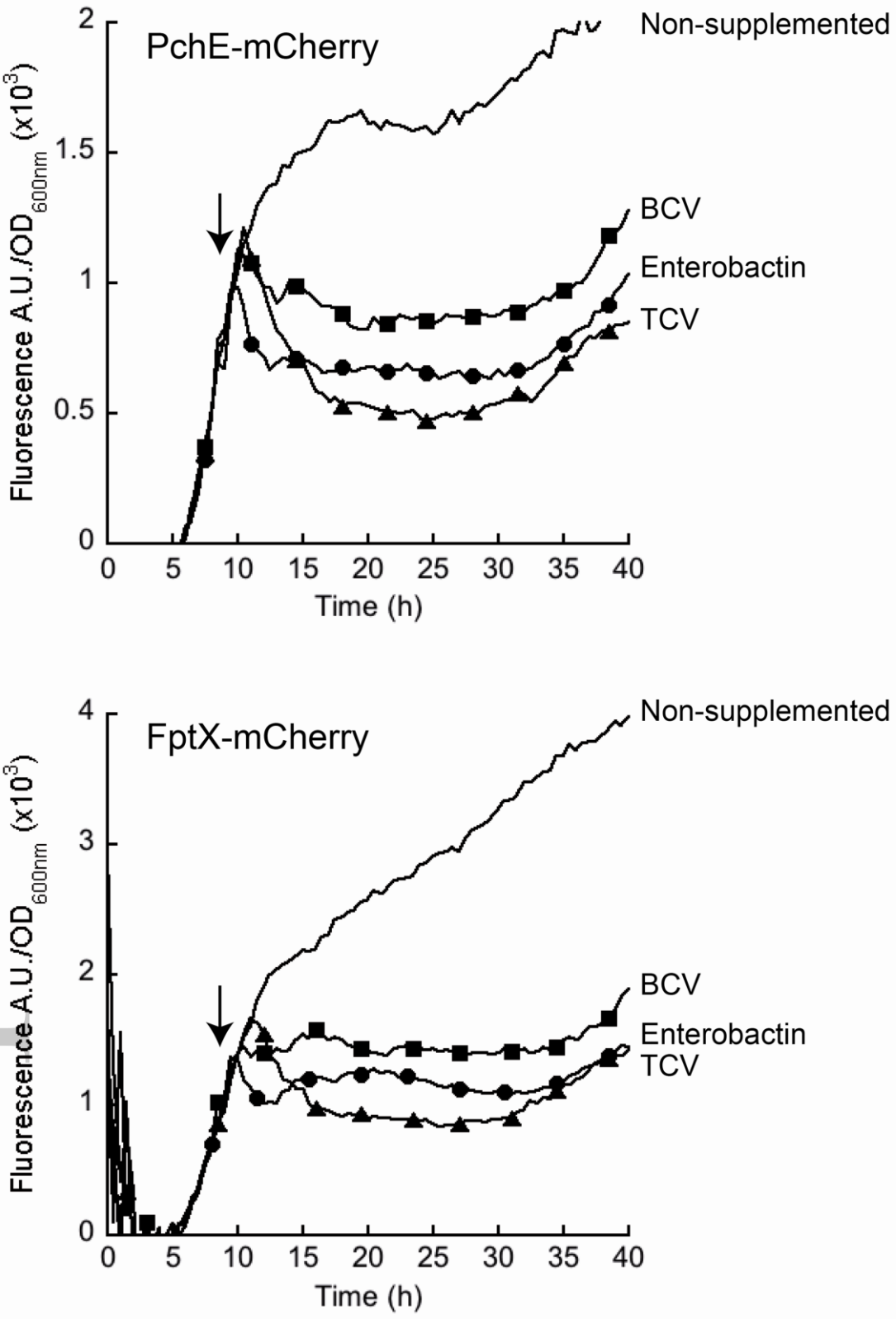

854

855 **EMI_13199_F7**